UC Irvine
UC Irvine Previously Published Works

Title
Structure-function relationships of fetal ovine articular cartilage

Permalink
https://escholarship.org/uc/item/2b29w51h

Authors
Brown, Wendy E
DuRaine, Grayson D
Hu, Jerry C
et al.

Publication Date
2019-03-01

DOI
10.1016/j.actbio.2019.01.073

Peer reviewed

eScholarship.org Powered by the California Digital Library
University of California

Elsevier Editorial System(tm) for Acta Biomaterialia

Manuscript Draft

Manuscript Number:

Title: Structure-function Relationships of Fetal Ovine Articular Cartilage

Article Type: Full length article

Keywords: biomechanical; biochemical; characterization; functional adaptation

Corresponding Author: Dr. Kyriacos A Athanasiou, PhD, PE

Corresponding Author's Institution: University of California Irvine

First Author: Wendy E Brown, PhD

Order of Authors: Wendy E Brown, PhD; Grayson D DuRaine, PhD; Jerry C Hu, PhD; Kyriacos A Athanasiou, PhD, PE

Abstract: It is crucial that the properties of repair cartilages, including engineered neocartilage, match surrounding healthy cartilage to promote the functional restoration of a cartilage injury. To accurately assess the quality of neocartilage, it's properties must be evaluated against healthy native cartilage. Fetal ovine cartilage has emerged as a promising and translationally relevant cell source with which to engineer neocartilage, yet, it is largely non-characterized. The influence of biomechanics during articular cartilage development, as well as their potential impact on structure-function relationships in utero in motivates additional study of fetal cartilage. Toward providing cartilage tissue engineering design criteria and elucidating fetal cartilage structure-function relationships, 11 locations across four regions of the fetal ovine stifle were characterized. Locational and regional differences were found to exist. Although differences in GAG content were observed, compressive stiffness did not vary or correlate with any biochemical component. Tensile stiffness and strength of the patella were significantly greater than those of the medial condyle. Tensile modulus and UTS significantly correlated with pyridinoline content. More advanced zonal organization, intense collagen II staining, and greater collagen and pyridinoline contents in the trochlear groove and patella suggest that these regions exhibit a more advanced maturational state than others. Regional differences in functional properties and their correlations suggest that structure-function relationships emerge in utero. These data address the dearth of information of the fetal ovine stifle, may serve as a repository of information for cartilage engineering strategies, and may help elucidate functional adaptation in fetal articular cartilage.

Dear Editor,

We are excited to present the research article entitled “Structure-function Relationships of Fetal Ovine Articular Cartilage.”

Fetal ovine chondrocytes have emerged as a promising and translationally relevant cell source with which to engineer neocartilage. However, fetal ovine articular cartilage is largely non-characterized. The role of biomechanical stimuli in articular cartilage development and its influence on structure-function relationships further motivates study of fetal cartilage.

In light of this, we comprehensively characterized 11 locations across four regions of the fetal ovine stifle with the goal of providing a benchmark for cartilage engineering efforts and to elucidate structure-function relationships in fetal articular cartilage. Importantly, locational and regional differences in fetal ovine cartilage were found to exist.

The data presented in this manuscript suggest that endochondral ossification drives functional adaptation in articular cartilage and that functional adaptation begins *in utero*, much earlier than previously thought. These data may clarify the order of development of cartilage functional properties. We anticipate that this study will be of broad interest to the *Acta Biomaterialia’s* readership.

We believe the following individuals will offer expertise in the review of this manuscript:

Corey Neu
Department of Mechanical Engineering
University of Colorado Boulder
cpneu@colorado.edu
(303) 492-7330

Johnna Temenoff
Department of Biomedical Engineering
Georgia Institute of Technology
johnna.temenoff@bme.gatech.edu
(404) 385-5026

Robert Sah
Department of Bioengineering
University of California San Diego
rsah@ucsd.edu
(858) 534-0821

On behalf of all the authors, thank you for your consideration.
Wendy E. Brown

***Statement of Significance**

Engineered neocartilage must be evaluated against healthy native cartilage to determine its ability to promote cartilage restoration. While fetal ovine cartilage has emerged as a promising and translationally relevant cell source with which to engineer neocartilage, it is largely non-characterized. Therefore, 11 locations across four regions (medial condyle, lateral condyle, trochlear groove, and patella) of the fetal ovine stifle were characterized. Importantly, the resulting data show that fetal cartilage is not "blank," as previously thought, and suggest that functional adaptation begins *in utero*. Furthermore, this study provides quantitative information regarding the fetal ovine stifle, clarifies the order of development of cartilage functional properties, informs future cartilage engineering efforts, and elucidates functional adaptation in fetal articular cartilage.

Graphical Abstract

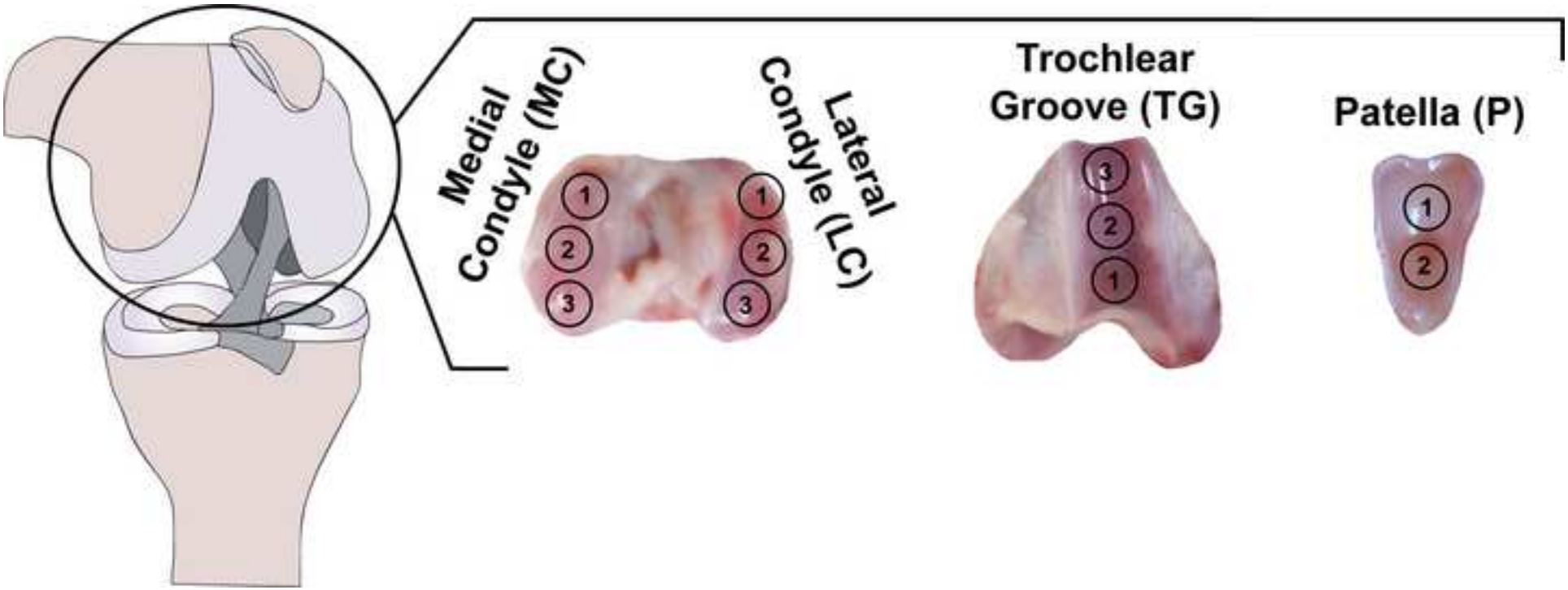

Manuscript File
Click here to view linked References

Structure-function Relationships of Fetal Ovine Articular Cartilage

Wendy E. Brown[a], Grayson D. DuRaine [b], Jerry C. Hu[c], Kyriacos A. Athanasiou[d,*]

[a]Department of Biomedical Engineering, University of California Irvine, 3120 Natural Sciences II Irvine, CA 92697-2715, USA. Email: wendy.brown@uci.edu.

[b]Department of Molecular Microbiology and Immunology, Oregon Health & Science University, 3181 SW Sam Jackson Park Road L220, Portland, OR 97239, USA. Email: duraine@ohsu.edu.

[c]Department of Biomedical Engineering, University of California Irvine, 3120 Natural Sciences II Irvine, CA 92697-2715, USA. Email: jerry.hu@uci.edu.

[d]Department of Biomedical Engineering, University of California Irvine, 3120 Natural Sciences II Irvine, CA 92697-2715, USA. Email: athens@uci.edu.

This work was supported by the National Institutes of Health R01 AR067821. The sponsor of this work had no role in the study design, the collection, analysis, and interpretation of data, writing of the report, or the decision to submit this article for publication.

Correspondence and reprint requests should be addressed to:
Athanasiou, KA
Department of Biomedical Engineering, University of California Irvine, 3120 Natural Sciences II Irvine, CA 92697-2715 USA
Tel.: (949) 432-2248
Fax: (949) 824-1727
Email: athens@uci.edu

No supplemental data has been included with this submission.

Abstract:

It is crucial that the properties of repair cartilages, including engineered neocartilage, match surrounding healthy cartilage to promote the functional restoration of a cartilage injury. To accurately assess the quality of neocartilage, it's properties must be evaluated against healthy native cartilage. Fetal ovine cartilage has emerged as a promising and translationally relevant cell source with which to engineer neocartilage, yet, it is largely non-characterized. The influence of biomechanics during articular cartilage development, as well as their potential impact on structure-function relationships *in utero* in motivates additional study of fetal cartilage. Toward providing cartilage tissue engineering design criteria and elucidating fetal cartilage structure-function relationships, 11 locations across four regions of the fetal ovine stifle were characterized. Locational and regional differences were found to exist. Although differences in GAG content were observed, compressive stiffness did not vary or correlate with any biochemical component. Tensile stiffness and strength of the patella were significantly greater than those of the medial condyle. Tensile modulus and UTS significantly correlated with pyridinoline content. More advanced zonal organization, intense collagen II staining, and greater collagen and pyridinoline contents in the trochlear groove and patella suggest that these regions exhibit a more advanced maturational state than others. Regional differences in functional properties and their correlations suggest that structure-function relationships emerge *in utero*. These data address the dearth of information of the fetal ovine stifle, may serve as a repository of information for cartilage engineering strategies, and may help elucidate functional adaptation in fetal articular cartilage.

Key Words: Biomechanical; Biochemical; Characterization; Functional Adaptation

1: Introduction

Articular cartilage repair therapies and cartilage tissue engineering efforts aim to restore function to damaged cartilage. To do so, repair cartilages, both innate and engineered, must withstand the arduous loading environments present within articulating joints. The knee, for example, experiences loads up to approximately 3.5 times bodyweight under a combination of compressive, tensile, and shear stresses [1]. Innate repair cartilage naturally formed in response to injuries frequently degenerates because it is mechanically inferior to the surrounding healthy cartilage [1]. Neocartilage has already been generated with not only mechanical properties but also organization that is reminiscent of healthy native tissue [2], making neocartilage implantation an appealing treatment for cartilage injuries. The properties of neocartilage may allow it to bear joint loading sooner after surgery than existing treatments, as well as impart the ability of neocartilage to integrate and promote repair in both small [3] and large [4] animal models. It is crucial that the properties of repair cartilage match those of the surrounding healthy cartilage to resist degeneration *in situ*, and ultimately, to promote the functional restoration of the injury site.

Histological analysis is frequently employed as the gold standard for assessing the quality of native, repair, and diseased articular cartilages. Indeed, the histological appearance of cartilage is considered to be one of the most important cartilage indicators [5]. To this end, qualitative and semi-quantitative, gross and histological analysis methods have been developed [6-11]. However, mechanical measurements may have greater sensitivity than histology for

subtle changes in cartilage quality. Though gross and histological examination may show only subtle differences in cartilage quality, these may reflect large differences in cartilage mechanical properties [12]. It has also been recommended that, regardless of the tissue type being evaluated, e.g., repair cartilage, osteoarthritic cartilage, or engineered neocartilage, histological scores are validated by comparison to quantitative biochemical evaluation [5]. Functionality indices that include both biochemical and mechanical parameters are also used to evaluate the quality of engineered neocartilages with respect to native cartilage [2, 13]. To fully determine the quality of repair cartilages, they must be assessed against healthy native cartilage by a complete set of histological and quantitative parameters, including biochemical, and mechanical assessments.

To perform accurate analysis of the quality of repair cartilage, it is essential to characterize healthy native cartilage of the relevant animal model. Native cartilage functional properties vary greatly with factors such as species, age, and location. For example, the aggregate modulus of the adult bovine lateral condyle greatly exceeds that of an adult rabbit, but the aggregate modulus of the adult leporine trochlear groove exceeds that of the adult cow [14]. Equine models exhibit age-dependent and topographical changes in mechanical properties [15]. A common translational model for cartilage repair, the ovine stifle, shows significant differences in both biochemical content and mechanical properties across different regions [16]. With the translational use of the ovine model in mind, fetal ovine cartilage is emerging as highly promising cell source for cartilage engineering, since fetal chondrocytes have high proliferative and matrix synthesis abilities [17, 18]. However, there is a dearth of knowledge of the quantitative functional properties of the fetal ovine stifle. Such information is required to

evaluate the quality of neocartilage engineered from a fetal ovine chondrocyte source. To provide benchmark functional properties for cartilage engineering efforts, it is necessary to characterize multiple locations within the articular cartilage of the species and age of animal model used, such as the translationally relevant fetal ovine stifle.

Cartilage biomechanics throughout development and maturation drive the emergence of topographical and regional variations in cartilage properties. The *in utero* mechanical environment acts as a regulator of stem cell fate and contributes to chondrogenesis and skeletogenesis. The balance of hydrostatic pressure, intermittent strain, and shear stresses direct the progression of the cartilage ossification front [19]. Biomechanical forces also promote cartilage maturation throughout fetal development and after birth. While cartilage mechanical properties are generally thought to change with developmental stage, loading patterns also drive topographical variations of functional properties in a process referred to as functional adaptation. For example, newborn and adult cartilage exhibits increased stiffness in areas bearing greater loads [15]. It has also been shown that cartilage from regions of the adult ovine stifle joints subjected to differing mechanical stresses contains chondrocyte populations of different phenotypes, as indicated by their relative synthesis of biglycan and decorin [20]. Several studies have shown that fetal cartilage is "blank,"[15] i.e., it does not show regional variations in biochemical content or mechanical properties. However, these studies are limited by the examination of only a few regions or by employing either histological examination, biochemical quantification, or mechanical analyses, but not all of them comprehensively. The importance and role of biomechanical stimuli in the development of articular cartilage *in utero* suggests these forces may also contribute to the cartilage's early functional adaptation,

motivating a comprehensive examination of fetal cartilage properties. Comprehensive characterization of fetal ovine stifle cartilage may shed light on the influence of biomechanical forces on cartilage developmental processes and early functional adaptation.

The objectives of this study were two-fold: 1) To provide a benchmark for cartilage engineering efforts that utilize fetal ovine cell sources, and 2) to provide missing data on the fetal ovine stifle toward elucidating functional adaptation of knee cartilage. This was accomplished by topographical and regional characterization of the articular cartilage of the fetal ovine stifle, including a comprehensive array of histological, biochemical, and mechanical assays. It was expected that characterizing 11 locations across four regions (medial condyle, lateral condyle, trochlear groove, and patella) of fetal cartilage would elucidate variations reflecting the influences of the biomechanical environment present during native cartilage formation.

2: Materials and Methods

2.1: Native Tissue Sample Preparation

The stifle joints of fetal (day 120 of ~150 day gestation) Dorper cross sheep were obtained as medical waste from the UC Davis School of Veterinary Medicine (Davis, CA) the day of sacrifice (n = 6). Samples from 11 topographical locations across four regions of the stifle (**Figure 1**) were immediately mechanically tested and preserved for histology. Additional samples from these locations were weighed and frozen for biochemical analysis. Samples were isolated from three locations on the medial condyle (MC), three locations on the lateral condyle (LC), three locations on the trochlear groove (TG), and two locations on the patella (P) by taking 5 mm

diameter punches from each location. These punches were then trimmed to a uniform thickness of 2.5 mm, with the articular surface intact, using a jig. Samples for compression testing were isolated by coring out a 3 mm diameter disc from the center of the 5 mm punch. The residual tissue not used for mechanical testing was then apportioned for histological and biochemical assays. Separate from the fetal tissues analyzed, juvenile ovine cartilage samples for the evaluation of crosslinks were obtained be removing the cartilage from the subchondral bone with a dermatome and trimming the pieces to uniform size, approximately 3 x 3 mm.

2.2: Gross Morphological Analysis

The exact dimensions of the stifle joint and cartilage samples were measured using ImageJ software (NIH) from photographs taken during sample preparation. Joint measurements were taken at the longest and/or widest points of each region.

2.3: Histological Evaluation

After fixation in 10% neutral buffered formalin, cartilage samples were dehydrated, embedded in paraffin, and sectioned to a thickness of 4 µm to expose the full thickness of the tissue. Sections were stained with Hematoxylin and Eosin to illustrate tissue and cell morphology, Safranin O/Fast Green to visualize glycosaminoglycans (GAGs), and Picrosirius Red to visualize collagen. Immunohistochemistry was also used to visualize collagen I (ab34710, 1:250 dilution, Abcam) and collagen II (ab34712, 1:4000 dilution, Abcam).

2.4: Biochemical Characterization

Samples were weighed to obtain wet weights, frozen and lyophilized, and weighed again to obtain dry weights. Lyophilized samples were digested in 125 µg/mL papain in phosphate buffer

at 60° C for 18 hours and assayed to determine biochemical content. A Blyscan dimethyl methylene blue assay kit (Biocolor, Ltd) was used to measure sulfated GAG content in the samples. A modified colorimetric chloramine-T hydroxyproline assay using hydrochloric acid [21] and a Sircol collagen assay standard (Biocolor, Ltd) was used to quantify collagen content. DNA content was measured by performing a Picogreen assay (Quant-iT Picogreen dsDNA assay kit). GAG and collagen contents were normalized to wet weight, dry weight, and DNA. High-performance liquid chromatography (HPLC) was performed to quantify pyridinoline crosslinks within fetal ovine cartilage, as well as juvenile ovine cartilage for reference. Lyophilized samples were digested in 4N HCl and dried in a vacuum concentrator. Digested samples were resuspended in 500 µL of a solution containing 1.67 nmol pyroxidine/mL, 8.3% acetonitrile, and 0.41% heptafluorobutyric acid (HFBA) in water. Resuspended samples were injected into a 25 mm C18 column (Shimadzu) and eluted using a modified solvent profile consisting of two solvents (1: 24% methanol and 0.13% HFBA in water and 2: 75% acetonitrile and 0.1% HFBA in water) [22]. Pyridinoline crosslinks were normalized to wet weight and total collagen content.

2.5: Mechanical Characterization

Creep indentation testing was performed by applying a 0.9 mm diameter, flat, porous indenter tip to the center of the 3 mm punches under a 0.5 N load to result in 8-10% sample strain. Values for the aggregate modulus, shear modulus, and permeability were obtained from the experimental data using a semi-analytical, semi-numerical, linear biphasic model and finite element analysis. [23] Uniaxial tensile testing was also performed. Using a jig, 5 mm diameter cartilage samples were trimmed into 1 mm thick layers still containing the articular surface. Samples were further trimmed into dog-bone shaped specimens with the long axis in the

direction of joint articulation and a gauge length of 2.34 mm, in adherence with ASTM standards (ASTM D3039). Paper tabs were glued to the specimens outside the gauge length and gripped in a TestResources uniaxial tester (TestResources Inc). The tabs were pulled parallel to the long axis of the specimen at a rate of 1% of the gauge length per second until sample failure. A stress-strain curve was generated using the cross-sectional area of samples measured with ImageJ. A least-squares fit of the linear region of the curve yielded the tensile modulus and the maximum stress achieved yielded the ultimate tensile strength (UTS).

2.6: Statistical Analysis

One-way analysis of variance tests (ANOVAs) followed by Tukey's *post hoc* tests were performed using Prism 7 software (GraphPad) on the quantitative data comparing the three topographical locations within the medial condyle, lateral condyle, and trochlear groove. Student's t-tests were performed comparing the two topographical locations on the patella. One-way ANOVAs with Tukey's *post hoc* tests on the combined data from each region were performed to compare data across the medial condyle, lateral condyle, trochlear groove, and patella regions. Two-way ANOVAs with Tukey's *post hoc* tests were used to analyze pyridinoline/WW and pyridinoline/collagen regional data. Correlations between mechanical properties (aggregate modulus, tensile modulus, and UTS) and biochemical contents (GAG/wet weight, collagen/wet weight, pyridinoline/wet weight, and pyridinoline/collagen) matched by location were detected by calculating Pearson correlation coefficients. Significance for all statistical analyses was determined by $p < 0.05$. Significantly different groups are indicated in figures by labeling with different letters.

3: Results

3.1: Gross Morphology

All cartilage appeared glossy and opaque white with visible vasculature underneath the translucent cartilage (**Figure 1**). The medial condyle was 38.9 ± 2.4 mm long and 15.9 ± 1.2 mm wide. The lateral condyle was 39.8 ± 1.3 mm long and 16.8 ± 0.8 mm wide. The trochlear groove was 46.2 ± 2.9 mm long and 25.7 ± 0.3 mm wide. The patella was 41.9 ± 1.4 mm long and 29.8 ± 1.1 mm wide.

3.2: Histology

Histological and immunohistochemical staining is shown in **Figure 2**. All topographical locations were densely populated with chondrocytes and showed vasculature. In the MC1, MC2, and MC3 locations, vascularization was present 668 ± 157, 485 ± 10, and 558 ± 219 µm below the surface, respectively. In the LC1, LC2, and LC3 locations, vascularization was present 496 ± 147, 519 ± 17, and 488 ± 82 µm below the articular surface, respectively. In the TG1, TG2, and TG3 locations, vascularization was present 490 ± 119, 596 ± 49, and 496 ± 28 µm below the articular surface, respectively. In the P1 and P2 locations, vascularization was present 485 ± 36 and 518 ± 10 µm below the articular surface, respectively. A tidemark or calcified osteochondral transitional region was not present. Chondrocytes near the articular surface were elongated with their long axis parallel to the surface and organized as single cells spaced 20-30 µm apart. Approximately 50 µm below the surface, chondrocytes appeared rounded and remained as individual cells or pairs of cells in close proximity (5-10 µm) to each other. Individual cells or pairs were spaced 20-30 µm apart with random organization. Within approximately 100-800

μm below the surface, chondrocytes appeared as either individual cells or pairs of cells within lacunae, and the space between single or paired cells increased to 40-50 μm, with some large gaps up to 80 μm. Beyond approximately 800 μm below the articular surface, cell density increased, and lacunae became larger. The presence of more distinct zones and large lacunae containing multiple chondrocytes were most evident in the patella and trochlear groove than in the medial or lateral condyle.

At all topographical locations, GAG staining was faint near the articular surface but increased with cartilage depth. Regionally, the lateral condyle stained most intensely for GAG, followed by the medial condyle, trochlear groove, and patella. Within each region, the locations with the most intense GAG staining were MC3, LC2, TG1, and P1, respectively. Total collagen staining was intense at the articular surface, faint below the surface, and more intense with increasing tissue depth for all locations. Collagen staining was similar between the medial and lateral condyle and slightly less intense in the patella. Collagen staining of the trochlear groove appeared much less intense than the other regions. Within the medial condyle, lateral condyle, trochlear groove, and patella, collagen staining was most intense at the MC2, LC2, TG1, and P2 locations, respectively. All locations stained minimally for collagen I, with the most intense staining occurring at the articular surface. All locations stained positively for collagen II, but with varying intensities. The trochlear groove stained most intensely for collagen II, followed by the medial condyle, lateral condyle, and patella. Within the medial condyle, lateral condyle, trochlear groove, and patella, collagen II staining was most intense at the MC2, LC3, TG1, and P1 locations, respectively.

3.3: Biochemical Content

A topographical analysis of biochemical content within each region is shown in **Table 1**. Notably, the GAG/DNA content of the MC3 location was significantly greater than that of the MC1 location. The GAG/wet weight content of the TG1 location was significantly greater than that of the TG3 location. GAG/dry weight contents of the MC1, MC2, and MC3 locations were 27.2 ± 5.1, 29.8 ± 4.3, and 32.5 ± 8.0%, respectively. GAG/dry weight contents of the LC1, LC2, and LC3 locations were 34.0 ± 7.4, 37.2 ± 3.8, and 37.4 ± 3.6%, respectively. GAG/dry weight contents of the TG1, TG2, and TG3 locations were 35.6 ± 9.0, 33.2 ± 6.4, and 32.1 ± 14.7%, respectively. GAG/dry weight contents of the P1 and P2 locations were 32.9 ± 8.5 and 27.7 ± 2.8%, respectively. Collagen/dry weight contents of the MC1, MC2, and MC3 locations were 53.5 ± 8.3, 56.8 ± 11.8, and 51.5 ± 6.7%, respectively. Collagen/dry weight contents of the LC1, LC2, and LC3 locations 63.4 ± 19.8, 68.3 ± 25.3, and 58.1 ± 11.6%, respectively. Collagen/dry weight contents of the TG1, TG2, and TG3 locations were 45.0 ± 8.4, 47.0 ± 9.4, and 52.1 ± 13.4%, respectively. Collagen/dry weight contents of the P1 and P2 locations were 56.7 ± 7.4 and 62.4 ± 15.0%, respectively.

A regional comparison of biochemical content is shown in **Figure 3**. Collagen/dry weight contents in the patella and lateral condyle were significantly greater than that of the trochlear groove. Additionally, a topographical examination of pyridinoline crosslinks within juvenile ovine articular cartilage was performed for reference. Pyridinoline/wet weight contents of the juvenile ovine MC1, MC2, and MC3 locations were 197.2 ± 7.8, 148.0 ± 14.1, and 170.8 ± 11.0 nmol/g, respectively. The pyridinoline/wet weight content of the MC1 location significantly exceeded that of the MC2 location. Pyridinoline/wet weight contents of the LC1, LC2, and LC3

locations were 191.3 ± 44.5, 252.6 ± 44.2, and 159.2 ± 6.3 nmol/g, respectively. Pyridinoline/wet weight contents of the TG1, TG2, and TG3 locations were 223.5 ± 15.5, 263.3 ± 118.7, and 249.9 ± 57.1 nmol/g, respectively. Pyridinoline/wet weight contents of the P1 and P2 locations were 330.7 ± 84.1 and 200.3 ± 26.5 nmol/g, respectively. Pyridinoline/collagen contents of the MC1, MC2, and MC3 locations were 1.1 ± 0.1, 0.9 ± 0.2, and 14. ± 0.3 nmol/mg, respectively. Pyridinoline/collagen contents of the LC1, LC2, and LC3 locations were 1.1 ± 0.3, 1.8 ± 0.5, and 1.3 ± 0.5 nmol/mg, respectively. Pyridinoline/collagen contents of the TG1, TG2, and TG3 locations were 3.2 ± 2.1, 1.8 ± 0.8, and 1.7 ± 0.7 nmol/mg, respectively. Pyridinoline/collagen contents of the P1 and P2 locations were 1.5 ± 0.7 and 1.9 ± 0.2 nmol/mg, respectively.

3.4: Mechanical Properties

A topographical analysis of mechanical properties within each region is shown in **Table 2**. A regional comparison of mechanical properties is shown in **Figure 4**.

3.5: Structure-Function Relationships

Mechanical properties (aggregate modulus, tensile modulus, and UTS) were each examined to determine their correlations with biochemical contents (GAG/wet weight, collagen/wet weight, pyridinoline/wet weight, and pyridinoline/collagen) (**Figure 5**). Tensile modulus significantly correlated positively with pyridinoline/wet weight and pyridinoline/collagen contents. UTS significantly correlated positively with collagen/wet weight, pyridinoline/wet weight, and pyridinoline/collagen contents.

4: Discussion

The goals of this study were to establish quantitative benchmark data for cartilage engineering efforts that use fetal ovine chondrocytes and to enhance the understanding of cartilage functional adaptation by comprehensively characterizing the articular cartilage of the fetal ovine stifle. Despite the prominence of the ovine model for translational cartilage repair and tissue engineering studies, the fetal ovine stifle has not yet been examined. Additionally, the emerging use of fetal chondrocytes for cartilage engineering further motivates the study of fetal cartilage properties [24]. Based on the importance of biomechanics-driven development *in utero* [19], it was expected that locational or regional differences in fetal ovine cartilage properties would exist and elucidate early functional adaptation. This hypothesis was supported by the data; significant differences among anatomical regions were observed histologically, biochemically, and mechanically (**Figures 2, 3, 4**). Furthermore, significant differences in biochemical content and mechanical properties were observed among topographical locations within regions (**Tables 1 and 2**). Tensile properties were observed to be significantly correlated with pyridinoline contents (**Figure 5**). In contrast to prior work in fetal bovine and equine models, regional patterns of biochemical and mechanical properties of fetal ovine cartilage were observed to match those previously reported for ovine cartilage of older animals [16]. The sequence of development of ECM components and mechanical properties parallels that seen during *in vitro* cartilage formation [1]. This study represents the first comprehensive characterization of fetal cartilage. Additionally, as the first effort to examine the articular cartilage of fetal ovine stifle, these data serve as a basis for evaluating the quality of *in*

vitro engineered cartilages. These data address the dearth of knowledge of the fetal ovine stifle and yield new perspectives on the functional adaptation and maturation of articular cartilage.

The comprehensive characterization of fetal sheep cartilage establishes a full data set to serve as the gold standard for cartilage engineering efforts. While the use of fetal ovine chondrocytes for cartilage engineering is desirable [17, 18], the fetal ovine stifle was largely non-characterized prior to this study. Histological, biochemical, and mechanical data were obtained from 11 locations throughout the four regions of the fetal sheep stifle, since all of these evaluations are crucial to fully understand cartilage quality [5, 12]. The data collected in this study may now be used to evaluate repair cartilages using quantitative systems and functionality indices [2, 10, 11, 13]. Quantitative evaluation of neocartilage against healthy native tissue aids in identifying engineering successes and shortcomings, ultimately advancing cartilage engineering efforts. The quantitative data obtained from this study may serve as a repository of information with which to evaluate neocartilage engineered from fetal ovine chondrocytes and further guide engineering strategies.

Region-based, histological differences were observed within fetal ovine articular cartilage. Vasculature was closest to the surface in the patella and trochlear groove regions, although not significantly so. While no tidemark was present, the precursors of cartilage zones were observed (**Figure 2**). The preliminary development of distinct zones was most defined in the patella and trochlear groove, suggesting more advanced maturation in these regions. The lateral condyle stained most intensely for GAG, mirroring the lateral condyle containing the most GAG/wet weight (**Figure 3**). Collagen staining was uniform across the medial and lateral condyles (**Figure 2**), analogous to the collagen/wet weight content in the medial and lateral

condyles (**Figure 3**). However, collagen II staining was most intense in the trochlear groove and patella. During cartilage development, other collagens, such as type VI [25, 26], are prevalent within fetal cartilage and localize to the pericellular matrix prior to increased collagen II production [26]. Therefore, the bulk of collagen staining in other regions may be due to collagen VI. The more advanced development of cartilage zones and the presence of intense collagen II staining in the trochlear groove and patella suggest that these regions are the first to mature, and, for the first time, suggest that different regions of the fetal knee exhibit different degrees of cartilage maturation.

By the mid-third trimester, fetal ovine cartilage was observed to contain GAG content on par with juvenile sheep (**Figures 4**) [16]. This pattern has also been observed in the bovine model [27]. The GAG/dry weight content of fetal ovine cartilage measured in this study was in the same range as that of fetal (mid-third trimester), calf (1-3 weeks), and adult (2 years) cows [27]. Thus, in concordance with previous studies, this study also shows that GAG content stays relatively constant with age [27, 28]. Additionally, for the first time, this study shows regional and locational differences in GAG content (**Figure 3** and **Table 1**). The regional pattern of GAG content observed in fetal cartilage mirrors the pattern of the aggregate modulus in juvenile ovine cartilage [16]. This suggests that the regional pattern of GAG content predicts future compressive properties and perhaps signals the onset of structure-function relationships.

Fetal compressive stiffness was found not to vary. The aggregate modulus of fetal ovine cartilage was observed to exceed that of fetal bovine cartilage [27], suggesting that the sheep may functionally mature earlier than the cow. Furthermore, fetal ovine compressive stiffness was found to be on par with juvenile ovine cartilage [16] (**Figure 4**). In juvenile ovine cartilage,

the lateral condyle and trochlear groove are significantly stiffer in compression than other regions [16]. In adult sheep, maximum joint loading (74% of the load) is borne by the medial condyle [29]. Sites of continuous loading become stiffer in compression with age [15]. Though loading studies have not been conducted in fetal and juvenile sheep, the implication may be that medial condyle cartilage should be the stiffest. This further suggests that functional adaptation of ovine cartilage progresses beyond the juvenile age and may involve more than just GAG content. Although it is commonly accepted that compressive stiffness is derived from cartilage's GAG content [30], this property may be influenced by other matrix components, such as collagen[27] and pyridinoline [31]. It has also been suggested that compressive stiffness is influenced by the interaction and organization of matrix components [32, 33]. It is, therefore, notable that, in the present study, the aggregate modulus of fetal ovine cartilage did not correlate individually with GAG, collagen, or pyridinoline contents (**Figure 5**). While the GAG content of fetal ovine cartilage is present at mature levels, the collagen and pyridinoline contents measured here are still well below those seen in juvenile and adult cartilage [16]. The larger mechanical forces experienced by articular cartilage after birth may stimulate cartilage maturation by production of collagen and pyridinoline [34, 35], and subsequently allow for matrix interactions that more clearly define functional relationships between compressive stiffness and biochemical contents. Correlations between compressive stiffness and individual biochemical contents are not evident in fetal ovine cartilage, but such structure-function relationships may become clear with the further development and interaction of matrix components.

While levels of collagen and pyridinoline crosslinking in fetal ovine cartilage are well below levels in more mature cartilage, age-independent patterns emerge. Values measured for fetal ovine cartilage in this study were on par with fetal bovine cartilage's collagen/dry weight [27, 36] and pyridinoline/wet weight [27, 36]. In contrast to the consistency of GAG content throughout age, collagen and pyridinoline contents of fetal ovine cartilage (**Figure 3**) were an order of magnitude lower than in juvenile ovine cartilage [16]. Despite differences in absolute values, the regional patterns of pyridinoline content in fetal ovine cartilage mirror those of juvenile ovine cartilage: pyridinoline/wet weight and pyridinoline/collagen contents trended higher in the trochlear groove and patella at both ages [16, 36]. The establishment of greater crosslinking in the patellofemoral groove of fetal cartilage, a pattern that remains consistent to maturity, has also been observed in the bovine model [36]. These results follow the histological signs of maturation observed in this study and discussed above. This study concurs with prior observations that the establishment of collagen content and pyridinoline crosslinks requires a longer maturation time than GAG content. Previous studies have shown that collagen and pyridinoline contents continue to increase through 2 years of age [36] to physiological maturity [37]. Additional studies examining the development of pyridinoline content from fetus to beyond skeletal maturity in the distinct locations studied here should be conducted to fully understand the timing of cartilage maturity and how crosslinking contributes to the establishment of cartilage mechanical properties and structure-function relationships.

Although the properties of fetal and neonatal cartilage are considered to be uniform, significant regional differences in tensile properties of fetal ovine cartilage were observed in this study. Prior studies have shown that mechanical properties and biochemical content of

equine and bovine fetal and neonatal cartilage do not differ among locations [15, 27, 36]. However, in this study, the tensile modulus and UTS values of the fetal patella were 73% and 65% greater than those of the medial condyle (**Figure 4**). It is possible that differences in functional properties are more evident in this study because of the greater number of locations examined than previous studies (11 versus two). Alternatively, it is known that compressive, tensile, and shear forces are present and have profound effects *in utero* [19, 38, 39]. Increased production of aggrecan and collagen II are associated with intermittent hydrostatic pressure [40]. Chondrocyte hypertrophy, production of collagen X, and zonal development are associated with endochondral ossification and are elicited by tensile and shear strain [40, 41]. The balance of these forces is what dictates the progression of the ossification front [19]. When hydrostatic pressure and shear stress were applied to contour plots of a knee, an osteogenic center were predicted to appear close to the surface and in the center of a concave joint surface [40], i.e., the trochlear groove. This supports the observation in this study that the trochlear groove and the opposing patella, which exhibit more distinct cartilage zones, strong collagen II staining, greater pyridinoline content and greater tensile properties, exhibit advanced maturation compared to other regions. The balance of biomechanical forces cartilage experiences *in utero* which drive endochondral ossification and cartilage maturation also may elicit regional differences in tensile properties and provide further evidence that the trochlear groove and patella regions mature first.

In contrast to the absence of compressive structure-function relationships, tensile structure-function relationships in fetal ovine cartilage are evident in this study. While collagen content is considered to be the main contributor to tensile properties, it has been shown more

recently that the degree of pyridinoline crosslinking within the collagen network also greatly contributes to tensile properties [42-44]. Significant, positive correlations between tensile properties and both collagen/wet weight and pyridinoline/wet weight have been reported for bovine cartilage samples combined from fetal, calf, and adult sources. However, these correlations were not detected within only fetal cartilage samples [36]. In this study, tensile modulus significantly correlated positively with both pyridinoline/wet weight and pyridinoline/collagen contents. UTS significantly correlated positively with pyridinoline/collagen content (**Figure 5**). This implies that the mechanical stimulation experienced *in utero* already elicits functional adaptation, which also occurs much earlier than previously thought [15, 45]. While this is not the first time that crosslinking has been explored in fetal cartilage [27, 36], this study represents the first examination of these characteristics in fetal ovine cartilage, the first evidence of functional adaptation *in utero*, and the first time pyridinoline-related maturation has been shown to vary regionally within a developing joint. Clearly defined structure-function relationships between tensile properties and pyridinoline crosslinks suggest that functional adaptation of cartilage occurs much earlier than previously thought.

By combining the data obtained in this study with previous studies of cartilage in older animals, it may be possible to delineate cartilage maturation pathways. In terms of the development of cartilage ECM components, GAG content may be established first. In this study, GAG content was observed to be on par with that of juvenile tissue at the mid-third trimester [16]. This level of GAG content is maintained without much variation throughout life.[27, 28] This abundance of GAG imparts compressive stiffness to fetal cartilage that is also on par with that of juvenile cartilage [16]. However, in fetal cartilage, the regional differences in aggregate

moduli reported for juvenile cartilage were not observed. Additionally, expected structure-function relationships were not yet evident, as aggregate modulus was observed not to correlate with GAG, collagen, or pyridinoline contents. Despite mature levels of GAG content, collagen and pyridinoline contents in fetal cartilage were well below those previously reported for juvenile ovine cartilage [16]. The lack of correlations between compressive properties and individual biochemical contents supports evidence that matrix components other than GAG, such as pyridinoline [31], or the interaction of matrix components within a mature ECM, play a role in establishing mature patterns of compressive properties and structure-function relationships [32], Next to develop in the ECM may be collagen, followed by pyridinoline. Collagen and pyridinoline contents have been shown to increase through 2 years of age in bovine articular cartilage [36], After collagen synthesis and collagen fiber assembly, LOX may induce the formation of pyridinoline crosslinks between collagen fibers, stabilizing the formation of heterotypic fibers, and therefore the ECM as a whole [44]. Concomitant with the increase in crosslinking is an increase in cartilage tensile properties [36]. In this study, significant correlations between tensile properties and pyridinoline contents were detected. This is likely due to the strong contribution of crosslinking to cartilage tensile properties, versus the contribution of multiple matrix components to compressive properties. By combining the insights gained from this work with previous studies of cartilage development, a clearer picture of the sequence of events that give rise to cartilage's salient properties emerges.

Scaffold-free cartilage tissue engineering methods are reminiscent of the cartilage developmental progressions elucidated in the present study. Articular cartilage engineered with the self-assembling process develops in phases [46]. In the first phase, cells are seeded at a high

density into non-adherent agarose wells to prevent cellular adhesion to the substrate and encourage cellular interactions. This phase is reminiscent of mesenchymal condensation that takes place during developmental chondrogenesis [47]. In the second phase, free energy is minimized as N-cadherin mediated cell-to-cell interactions take place, resulting in neocartilage formation. In native cartilage development, N-cadherin plays an important role in early condensation [48]. In the third phase, collagen VI and high levels of GAG, specifically chondroitin-6-sulphate, are synthesized [46]. GAG levels increase to native-tissue levels and plateau within 4 weeks [49]. Similarly, GAG content within fetal cartilage is established early, as levels *in utero* are on par with juvenile cartilage [16, 27]. In the fourth phase of self-assembly, collagen VI localizes to the pericellular matrix, collagen II production increases, and chondroitin-6-sulphate:chondroitin-4-sulphate ratio decreases, all paralleling developmental processes [25, 26, 28, 49, 50]. These biochemical components impart a nascent level of compressive and tensile characteristics in engineered neocartilage; however, collagen content and pyridinoline crosslinking remain below the levels of mature native tissue [16, 36, 43]. This implies that neocartilage is engineered with this method has yet to complete maturation. Recently identified structure-function relationships show the importance of pyridinoline crosslinks to not only tensile properties but also compressive properties [27, 36, 43]. The exogenous treatment of neocartilage with LOXL2, an enzyme that creates pyridinoline crosslinks within the collagen network, may recapitulate pyridinoline-associated maturation in native cartilage development [44]. The “order of operations” of cartilage development elucidated in this study is replicated in neocartilage development, often to native cartilage levels, lending further credence to the self-assembling process as an *in vitro* model of cartilage formation and development.

In summary, this study yielded a quantitative understanding of the articular cartilage of the fetal ovine stifle, and in doing so, elucidated the development of structure-function relationships and functional adaptation. It was shown that fetal cartilage is not mechanically "blank." In general, the GAG content and aggregate modulus of fetal cartilage were on par with those of juvenile cartilage. No significant structure-function correlations could be identified between aggregate modulus and any biochemical component within fetal cartilage. However, regional patterns of GAG content in fetal cartilage matched regional patterns of compressive properties in juvenile ovine cartilage, suggesting that these GAG differences are predictive of compressive properties in matured cartilage. While collagen content, pyridinoline content, and tensile properties of fetal cartilage were much lower than in more mature cartilage, clear structure-function relationships were illustrated with respect to tensile properties. Tensile modulus and UTS were correlated to pyridinoline content, further supporting recent evidence that not only collagen content, but also crosslinking greatly contributes to tensile properties. These data suggest that functional adaptation in articular cartilage begins *in utero*, much earlier than previously thought, as a product of the forces that drive endochondral ossification. The trochlear groove and patella exhibited the greatest pyridinoline content and tensile properties, providing further evidence of more advanced maturation in these areas. These observations, combined with previously reported studies of cartilage development, may clarify the order of development of cartilage functional properties and lend further credence to the self-assembling process as an *in vitro* model of cartilage development. These data also serve as a repository of information for fetal ovine cartilage, providing benchmark functional properties for tissue engineering efforts.

Acknowledgments

This work was supported by the National Institutes of Health R01 AR067821. The authors would also like to thank Drs. Diana Farmer, Aijun Wang, and Gary Raff for the generous donation of the fetal ovine stifle joints and Linda Talken for assistance in obtaining the tissues.

References

[1] K.A. Athanasiou, E.M. Darling, G.D. DuRaine, J.C. Hu, A.H. Reddi, Articular Cartilage, Second ed., CRC Press, Boca Raton, FL, 2017.

[2] R.F. MacBarb, A.L. Chen, J.C. Hu, K.A. Athanasiou, Engineering functional anisotropy in fibrocartilage neotissues, Biomaterials 34(38) (2013) 9980-9.

[3] G.D. DuRaine, B. Arzi, J.K. Lee, C.A. Lee, D.J. Responte, J.C. Hu, K.A. Athanasiou, Biomechanical evaluation of suture-holding properties of native and tissue-engineered articular cartilage, Biomech Model Mechanobiol 14(1) (2015) 73-81.

[4] P. Mainil-Varlet, F. Rieser, S. Grogan, W. Mueller, C. Saager, R.P. Jakob, Articular cartilage repair using a tissue-engineered cartilage-like implant: an animal study, Osteoarthr Cartilage 9 (2001) S6-S15.

[5] M. Rutgers, M.J. van Pelt, W.J. Dhert, L.B. Creemers, D.B. Saris, Evaluation of histological scoring systems for tissue-engineered, repaired and osteoarthritic cartilage, Osteoarthritis and cartilage / OARS, Osteoarthritis Research Society 18(1) (2010) 12-23.

[6] S.W. O'Driscoll, F.W. Keeley, R.B. Salter, The chondrogenic potential of free autogenous periosteal grafts for biological resurfacing of major full-thickness defects in joint surfaces under the influence of continuous passive motion. An experimental investigation in the rabbit, The Journal of bone and joint surgery. American volume 68(7) (1986) 1017-35.

[7] S. Pineda, A. Pollack, S. Stevenson, V. Goldberg, A. Caplan, A semiquantitative scale for histologic grading of articular cartilage repair, Acta Anat (Basel) 143(4) (1992) 335-40.

[8] G.D. Smith, J. Taylor, K.F. Almqvist, C. Erggelet, G. Knutsen, M. Garcia Portabella, T. Smith, J.B. Richardson, Arthroscopic assessment of cartilage repair: a validation study of 2 scoring systems, Arthroscopy : the journal of arthroscopic & related surgery : official publication of the Arthroscopy Association of North America and the International Arthroscopy Association 21(12) (2005) 1462-7.

[9] P. Mainil-Varlet, B. Van Damme, D. Nesic, G. Knutsen, R. Kandel, S. Roberts, A new histology scoring system for the assessment of the quality of human cartilage repair: ICRS II, Am J Sports Med 38(5) (2010) 880-90.

[10] S.W. O'Driscoll, R.G. Marx, D.E. Beaton, Y. Miura, S.H. Gallay, J.S. Fitzsimmons, Validation of a simple histological-histochemical cartilage scoring system, Tissue engineering 7(3) (2001) 313-20.

[11] S.P. Grogan, A. Barbero, V. Winkelmann, F. Rieser, J.S. Fitzsimmons, S. O'Driscoll, I. Martin, P. Mainil-Varlet, Visual histological grading system for the evaluation of in vitro-generated neocartilage, Tissue engineering 12(8) (2006) 2141-9.

[12] W. Waldstein, G. Perino, S.L. Gilbert, S.A. Maher, R. Windhager, F. Boettner, OARSI osteoarthritis cartilage histopathology assessment system: A biomechanical evaluation in the human knee, J Orthop Res 34(1) (2016) 135-40.

[13] B.D. Elder, K.A. Athanasiou, Systematic assessment of growth factor treatment on biochemical and biomechanical properties of engineered articular cartilage constructs, Osteoarthr Cartilage 17(1) (2009) 114-123.

[14] K.A. Athanasiou, M.P. Rosenwasser, J.A. Buckwalter, T.I. Malinin, V.C. Mow, Interspecies comparisons of in situ intrinsic mechanical properties of distal femoral cartilage, J Orthop Res 9(3) (1991) 330-40.

[15] H. Brommer, P.A. Brama, M.S. Laasanen, H.J. Helminen, P.R. van Weeren, J.S. Jurvelin, Functional adaptation of articular cartilage from birth to maturity under the influence of loading: a biomechanical analysis, Equine Vet J 37(2) (2005) 148-54.

[16] L.W. Huwe, W.B. Brown, K.A. Athanasiou, J.C. Hu, Characterization of costal cartilage and its suitability as a cell source for articular cartilage tissue engineering.

[17] W.H. Choi, H.R. Kim, S.J. Lee, N. Jeong, S.R. Park, B.H. Choi, B.H. Min, Fetal Cartilage-derived Cells have Stem Cell Properties and are a Highly Potent Cell Source for Cartilage Regeneration, Cell transplantation (2015).

[18] J.R. Fuchs, S. Terada, D. Hannouche, E.R. Ochoa, J.P. Vacanti, D.O. Fauza, Engineered fetal cartilage: structural and functional analysis in vitro, J Pediatr Surg 37(12) (2002) 1720-5.

[19] D.J. Responte, J.K. Lee, J.C. Hu, K.A. Athanasiou, Biomechanics-driven chondrogenesis: from embryo to adult, FASEB J 26(9) (2012) 3614-24.

[20] C.B. Little, P. Ghosh, Variation in proteoglycan metabolism by articular chondrocytes in different joint regions is determined by post-natal mechanical loading, Osteoarthritis and cartilage / OARS, Osteoarthritis Research Society 5(1) (1997) 49-62.

[21] D.D. Cissell, J.M. Link, J.C. Hu, K.A. Athanasiou, A Modified Hydroxyproline Assay Based on Hydrochloric Acid in Ehrlich's Solution Accurately Measures Tissue Collagen Content, Tissue engineering. Part C, Methods 23(4) (2017) 243-250.

[22] R.A. Bank, B. Beekman, N. Verzijl, J.A. de Roos, A.N. Sakkee, J.M. TeKoppele, Sensitive fluorimetric quantitation of pyridinium and pentosidine crosslinks in biological samples in a single high-performance liquid chromatographic run, J Chromatogr B Biomed Sci Appl 703(1-2) (1997) 37-44.

[23] K.A. Athanasiou, A. Agarwal, A. Muffoletto, F.J. Dzida, G. Constantinides, M. Clem, Biomechanical properties of hip cartilage in experimental animal models, Clinical orthopaedics and related research (316) (1995) 254-66.

[24] W.E. Brown, J.C. Hu, K.A. Athanasiou, Ammonium-Chloride-Potassium Lysing Buffer Treatment of Fully Differentiated Cells Increases Cell Purity and Resulting Neotissue Functional Properties, Tissue engineering. Part C, Methods 22(9) (2016) 895-903.

[25] D.R. Eyre, The collagens of articular cartilage, Semin Arthritis Rheum 21(3 Suppl 2) (1991) 2-11.

[26] E.H. Morrison, M.W. Ferguson, M.T. Bayliss, C.W. Archer, The development of articular cartilage: I. The spatial and temporal patterns of collagen types, J Anat 189 (Pt 1) (1996) 9-22.

[27] A.K. Williamson, A.C. Chen, R.L. Sah, Compressive properties and function-composition relationships of developing bovine articular cartilage, J Orthop Res 19(6) (2001) 1113-21.

[28] D. Platt, J.L. Bird, M.T. Bayliss, Ageing of equine articular cartilage: structure and composition of aggrecan and decorin, Equine Vet J 30(1) (1998) 43-52.

[29] W.R. Taylor, B.M. Poepplau, C. Konig, R.M. Ehrig, S. Zachow, G.N. Duda, M.O. Heller, The medial-lateral force distribution in the ovine stifle joint during walking, J Orthop Res 29(4) (2011) 567-71.

[30] V.C. Mow, A. Ratcliffe, Structure and function of articular cartilage and meniscus, Second ed., Lippincott-Raven Publishers1997.

[31] T. Ficklin, G. Thomas, J.C. Barthel, A. Asanbaeva, E.J. Thonar, K. Masuda, A.C. Chen, R.L. Sah, A. Davol, S.M. Klisch, Articular cartilage mechanical and biochemical property relations before and after in vitro growth, J Biomech 40(16) (2007) 3607-3614.

[32] S. Treppo, H. Koepp, E.C. Quan, A.A. Cole, K.E. Kuettner, A.J. Grodzinsky, Comparison of biomechanical and biochemical properties of cartilage from human knee and ankle pairs, J Orthop Res 18(5) (2000) 739-48.

[33] R.L. Sah, A.C. Chen, A.J. Grodzinsky, S.B. Trippel, Differential effects of bFGF and IGF-I on matrix metabolism in calf and adult bovine cartilage explants, Arch Biochem Biophys 308(1) (1994) 137-47.

[34] S.W. Verbruggen, J.H. Loo, T.T. Hayat, J.V. Hajnal, M.A. Rutherford, A.T. Phillips, N.C. Nowlan, Modeling the biomechanics of fetal movements, Biomech Model Mechanobiol 15(4) (2016) 995-1004.

[35] T.W. Flynn, R.W. Soutas-Little, Patellofemoral joint compressive forces in forward and backward running, J Orthop Sports Phys Ther 21(5) (1995) 277-82.

[36] A.K. Williamson, A.C. Chen, K. Masuda, E.J.M.A. Thonar, R.L. Sah, Tensile mechanical properties of bovine articular cartilage: variations with growth and relationships to collagen network components, J Orthop Res 21(5) (2003) 872-880.

[37] T. Moriguchi, D. Fujimoto, Age-related changes in the content of the collagen crosslink, pyridinoline, J Biochem 84(4) (1978) 933-5.

[38] K.A. Roddy, P.J. Prendergast, P. Murphy, Mechanical Influences on Morphogenesis of the Knee Joint Revealed through Morphological, Molecular and Computational Analysis of Immobilised Embryos, PloS one 6(2) (2011).

[39] B. Mikic, A.L. Isenstein, A. Chhabra, Mechanical modulation of cartilage structure and function during embryogenesis in the chick, Annals of biomedical engineering 32(1) (2004) 18-25.

[40] D.R. Carter, G.S. Beaupre, M. Wong, R.L. Smith, T.P. Andriacchi, D.J. Schurman, The mechanobiology of articular cartilage development and degeneration, Clinical orthopaedics and related research (427) (2004) S69-S77.

[41] H.M. Kronenberg, Developmental regulation of the growth plate, Nature 423(6937) (2003) 332-6.

[42] E.A. Makris, J.C. Hu, K.A. Athanasiou, Hypoxia-induced collagen crosslinking as a mechanism for enhancing mechanical properties of engineered articular cartilage, Osteoarthritis and cartilage / OARS, Osteoarthritis Research Society 21(4) (2013) 634-41.

[43] E.A. Makris, R.F. MacBarb, D.J. Responte, J.C. Hu, K.A. Athanasiou, A copper sulfate and hydroxylysine treatment regimen for enhancing collagen cross-linking and biomechanical properties in engineered neocartilage, FASEB J 27(6) (2013) 2421-30.

[44] E.A. Makris, D.J. Responte, N.K. Paschos, J.C. Hu, K.A. Athanasiou, Developing functional musculoskeletal tissues through hypoxia and lysyl oxidase-induced collagen cross-linking, Proceedings of the National Academy of Sciences of the United States of America 111(45) (2014) E4832-41.

[45] S. Akizuki, V.C. Mow, F. Muller, J.C. Pita, D.S. Howell, D.H. Manicourt, Tensile properties of human knee joint cartilage: I. Influence of ionic conditions, weight bearing, and fibrillation on the tensile modulus, J Orthop Res 4(4) (1986) 379-92.

[46] K.A. Athanasiou, R. Eswaramoorthy, P. Hadidi, J.C. Hu, Self-organization and the self-assembling process in tissue engineering, Annual review of biomedical engineering 15 (2013) 115-36.

[47] M. Pacifici, E. Koyama, M. Iwamoto, C. Gentili, Development of articular cartilage: what do we know about it and how may it occur?, Connective tissue research 41(3) (2000) 175-84.

[48] S.A. Oberlender, R.S. Tuan, Spatiotemporal profile of N-cadherin expression in the developing limb mesenchyme, Cell Adhes Commun 2(6) (1994) 521-37.

[49] G. Ofek, C.M. Revell, J.C. Hu, D.D. Allison, K.J. Grande-Allen, K.A. Athanasiou, Matrix development in self-assembly of articular cartilage, PloS one 3(7) (2008) e2795.

[50] C.W. Archer, E.H. Morrison, M.T. Bayliss, M.W. Ferguson, The development of articular cartilage: II. The spatial and temporal patterns of glycosaminoglycans and small leucine-rich proteoglycans, J Anat 189 (Pt 1) (1996) 23-35.

Location		Water Content (%)	GAG/ Wet Weight (%)	GAG/ DNA (μg/μg)	Collagen/ Wet Weight (%)	Collagen/ DNA (μg/μg)	Pyridinoline/ Wet Weight (nmol/g)	Pyridinoline/ Collagen (nmol/mg)	DNA/ Wet Weight (ng/μg)
Medial Condyle	**1**	85.6 ± 1.2	3.9 ± 0.9	92.3 ± 32.2^{B}	7.7 ± 1.4	196.9 ± 101.1	22.5 ± 17.1	0.33 ± 0.27	0.49 ± 0.25
	2	85.9 ± 0.6	4.2 ± 0.7	229.7 ± 146.0^{AB}	8.0 ± 1.9	482.5 ± 380.4	21.3 ± 16.0	0.35 ± 0.29	0.26 ± 0.17
	3	85.0 ± 1.4	4.8 ± 1.0	291.7 ± 143.6^{A}	7.7 ± 1.1	496.1 ± 348.4	16.8 ± 12.1	0.24 ± 0.20	0.22 ± 0.14
Lateral Condyle	**1**	86.1 ± 1.5	4.7 ± 1.1	276.9 ± 146.7	8.7 ± 2.5	549.4 ± 343.3	16.9 ± 11.0	0.3 ± 0.18	0.23 ± 0.16
	2	85.7 ± 1.0	5.3 ± 0.5	355.3 ± 207.1	8.7 ± 2.5	542.4 ± 467.1	30.3 ± 17.1	0.39 ± 0.25	0.15 ± 0.05
	3	86.8 ± 2.1	5.0 ± 0.9	455.5 ± 261.6	7.6 ± 1.5	761.0 ± 519.2	33.0 ± 18.1	0.50 ± 0.27	0.17 ± 0.14
Trochlear Groove	**1**	84.5 ± 2.8	5.7 ± 2.1^{A}	513.4 ± 245.8	6.9 ± 1.1	511.0 ± 224.9	33.6 ± 20.4	0.35 ± 0.22	0.12 ± 0.09
	2	86.2 ± 1.7	5.1 ± 0.5^{AB}	639.8 ± 552.7	6.5 ± 1.6	937.6 ± 982.4	32.9 ± 15.2	0.41 ± 0.19	0.14 ± 0.11
	3	87.3 ± 2.5	3.9 ± 1.3^{B}	193.4 ± 89.3	6.5 ± 1.6	300.3 ± 192.4	37.1 ± 21.9	0.59 ± 0.28	0.25 ± 0.22
Patella	**1**	86.4 ± 1.4	4.5 ± 1.2	339.7 ± 219.7	7.7 ± 1.4	629.4 ± 437.3	34.2 ± 16.1	0.49 ± 0.24	0.21 ± 0.17
	2	85.8 ± 1.2	3.9 ± 0.3	246.1 ± 142.6	9.7 ± 2.9	725.2 ± 499.8	30.5 ± 10.6	0.45 ± 0.15	0.22 ± 0.16

Table 1 – Topographical Biochemical Data: Complete biochemical characterization data from 11 topographical locations are shown as mean ± standard deviation. Statistics were calculated amongst topographical locations within the same region.

Location		Aggregate Modulus (kPa)	Shear Modulus (kPa)	Permeability E-15 (m^4/N·s)	Tensile Modulus (MPa)	UTS (MPa)
Medial Condyle	**1**	142.3 ± 55.0	83.8 ± 35.9	4.9 ± 1.4	6.5 ± 0.1	2.3 ± 0.6
	2	175.5 ± 65.6	100.4 ± 37.1	6.4 ± 4.4	7.1 ± 3.6	1.8 ± 0.9
	3	180.1 ± 60.5	106.6 ± 33.7	7.5 ± 5.7	5.2 ± 1.0	1.6 ± 0.8
Lateral Condyle	**1**	148.8 ± 61.7	88.2 ± 41.7	4.9 ± 2.5	5.0 ± 0.9	1.9 ± 1.0
	2	128.9 ± 29.6	78.8 ± 22.5	5.4 ± 1.7	8.1 ± 0.6	2.1 ± 0.2
	3	162.4 ± 42.7	95.9 ± 31.5	4.2 ± 1.4	8.0 ± 2.1	2.2 ± 0.7
Trochlear Groove	**1**	177.1 ± 39.3	106.2 ± 21.1	4.4 ± 2.0	7.9 ± 3.2	1.9 ± 0.9
	2	173.4 ± 44.5	103.0 ± 25.9	4.1 ± 1.7	11.1 ± 6.3	2.8 ± 1.2
	3	138.5 ± 34.5	81.0 ± 19.3	7.1 ± 5.9	8.2 ± 2.8	1.6 ± 0.4
Patella	**1**	156.6 ± 68.7	94.6 ± 45.8	5.5 ± 3.0^{A}	9.1 ± 3.3	2.6 ± 0.9
	2	196.5 ± 40.0	120.1 ± 24.7	2.4 ± 0.7^{B}	12.9 ± 4.4	3.4 ± 1.5

Table 2 – Topographical Mechanical Data: Complete mechanical characterization data from 11 topographical locations are shown as mean ± standard deviation. Statistics were calculated amongst topographical locations within the same region.

Figure 1

Click here to download high resolution image

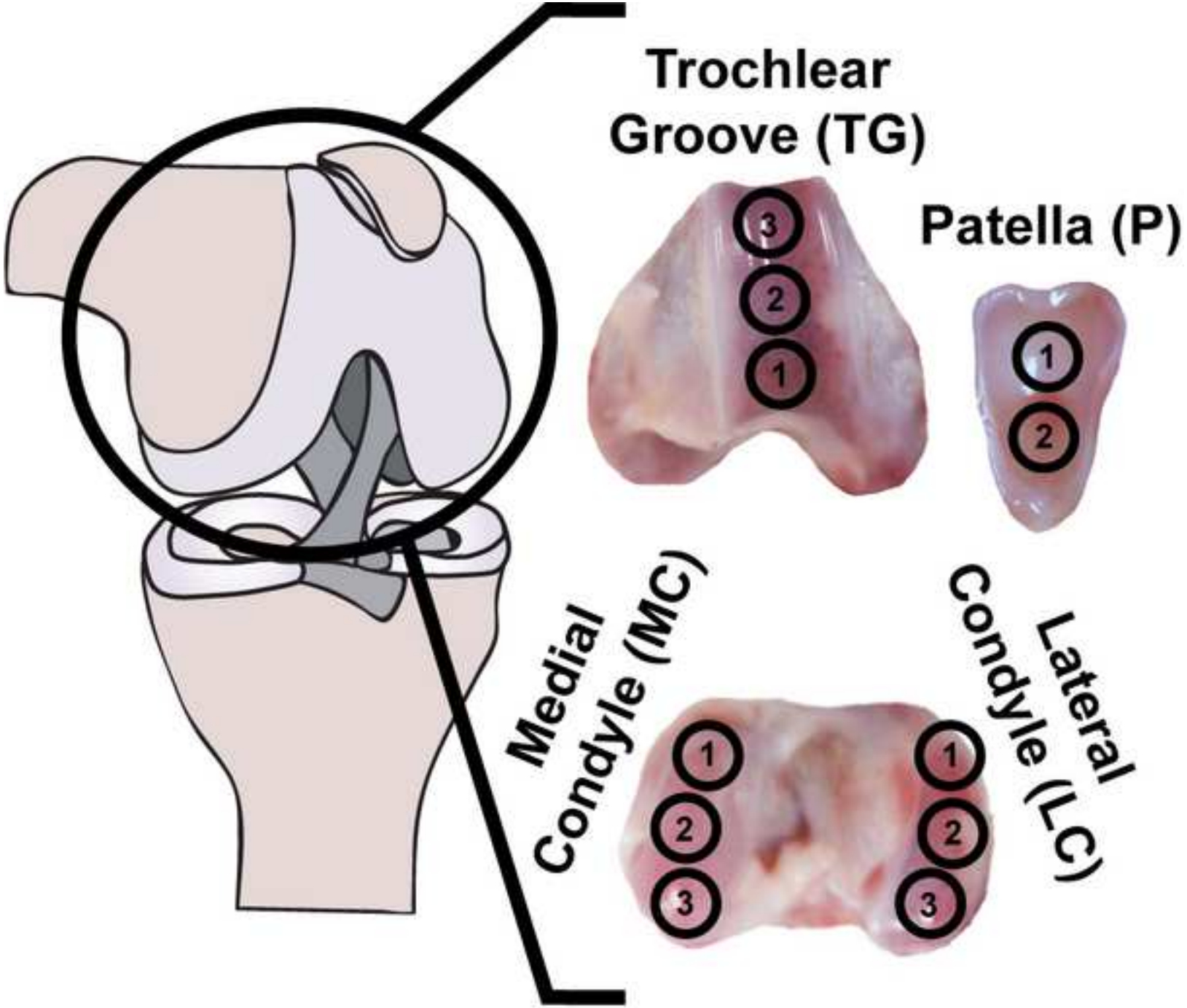

Figure 2

Click here to download high resolution image

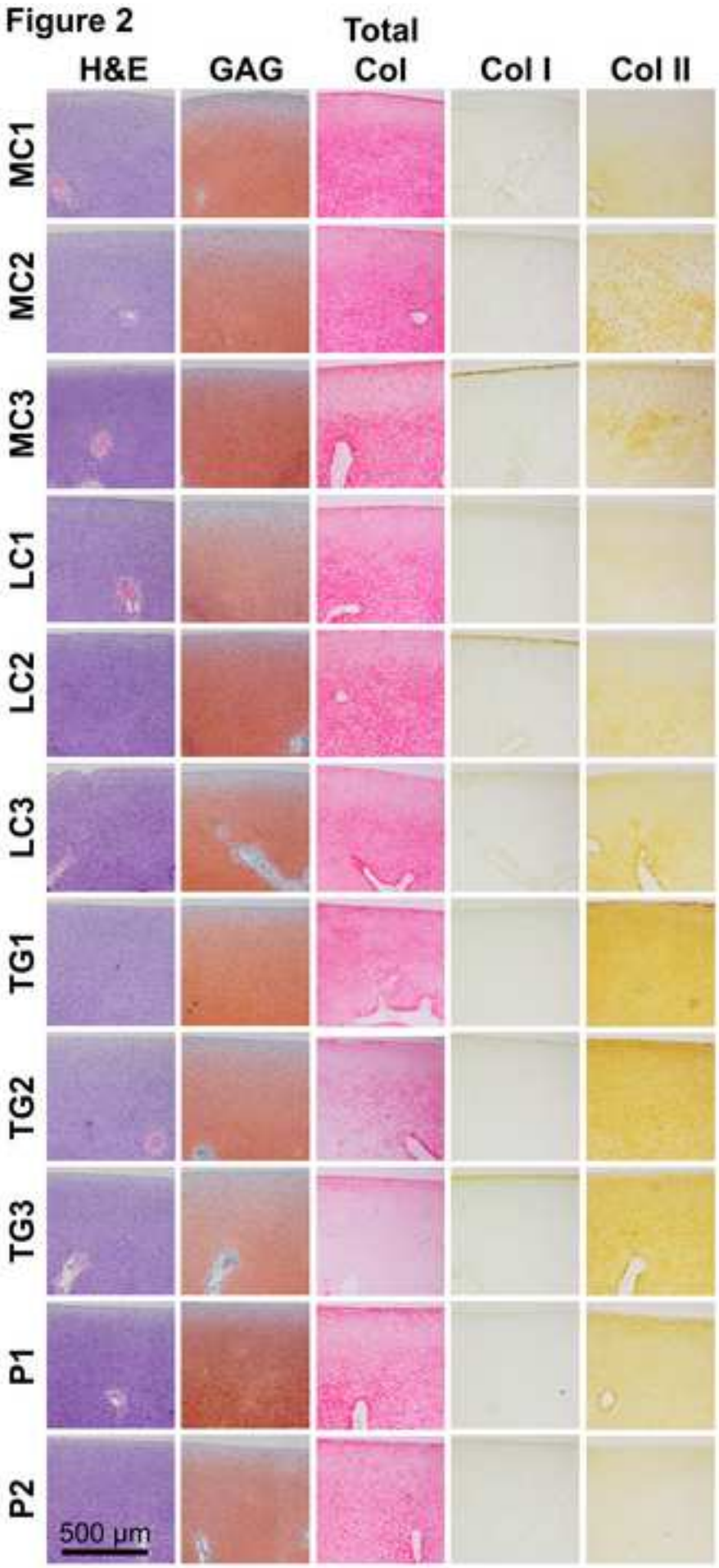

Figure 3

Click here to download high resolution image

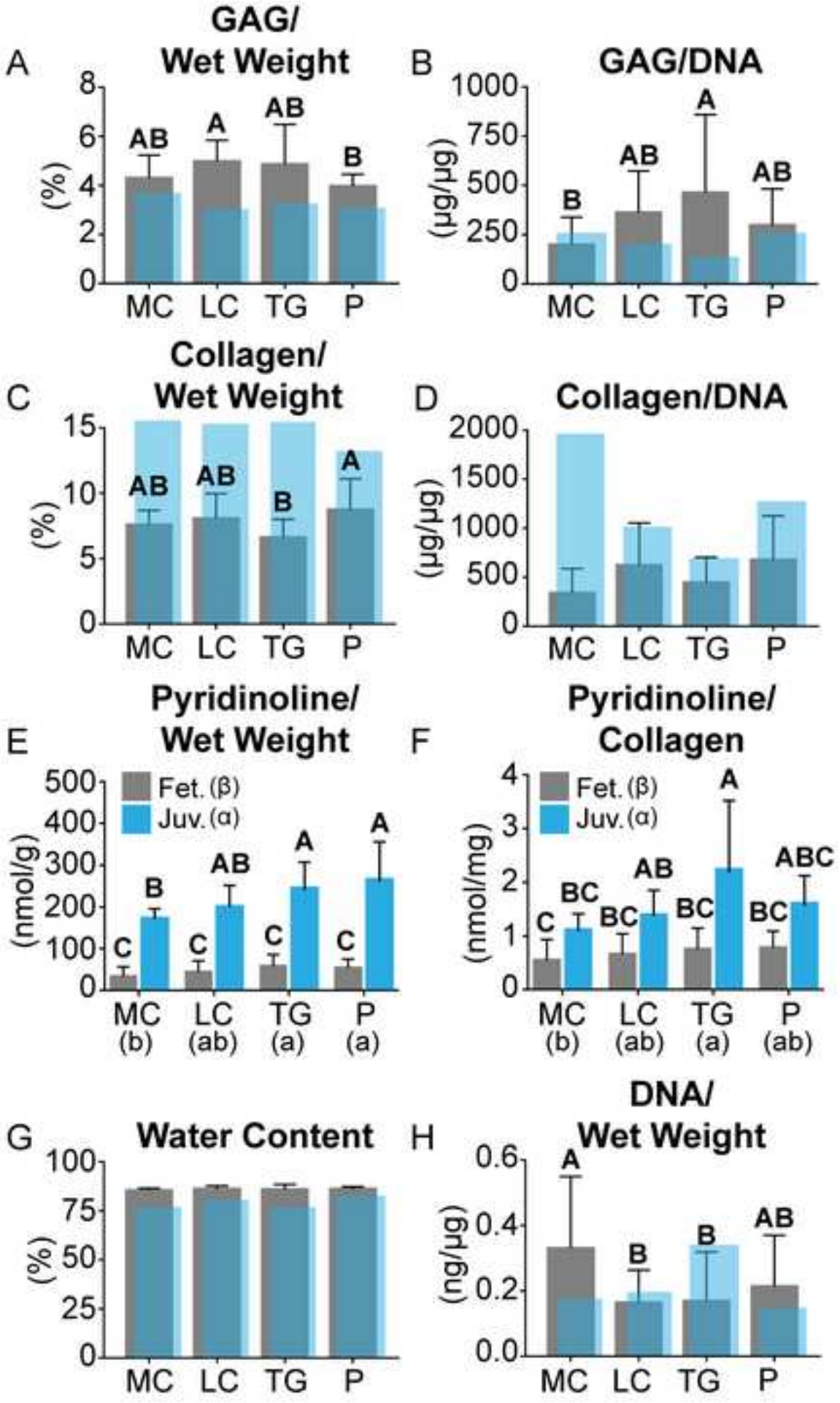

Figure 4

Click here to download high resolution image

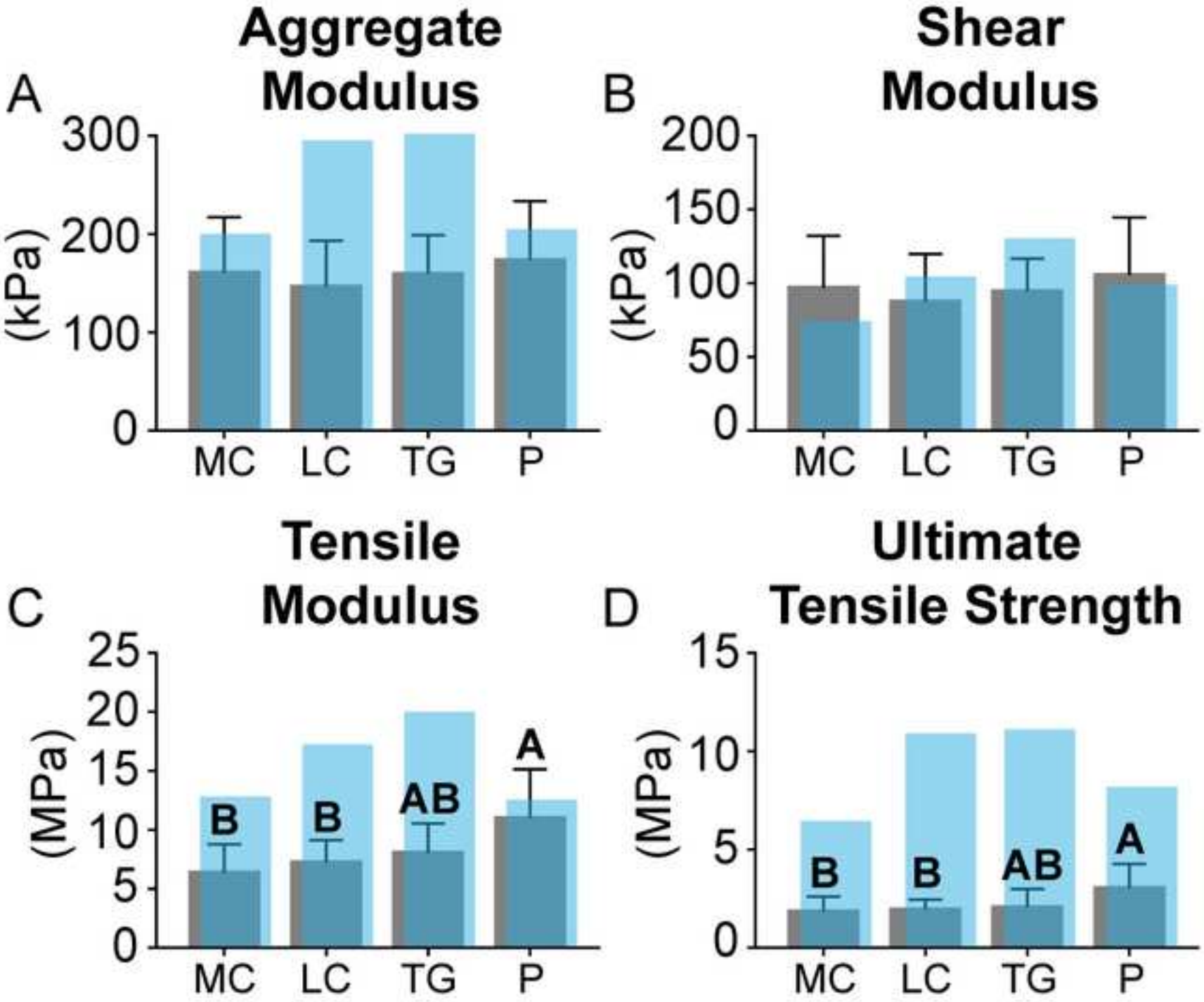

Figure 5

Click here to download high resolution image

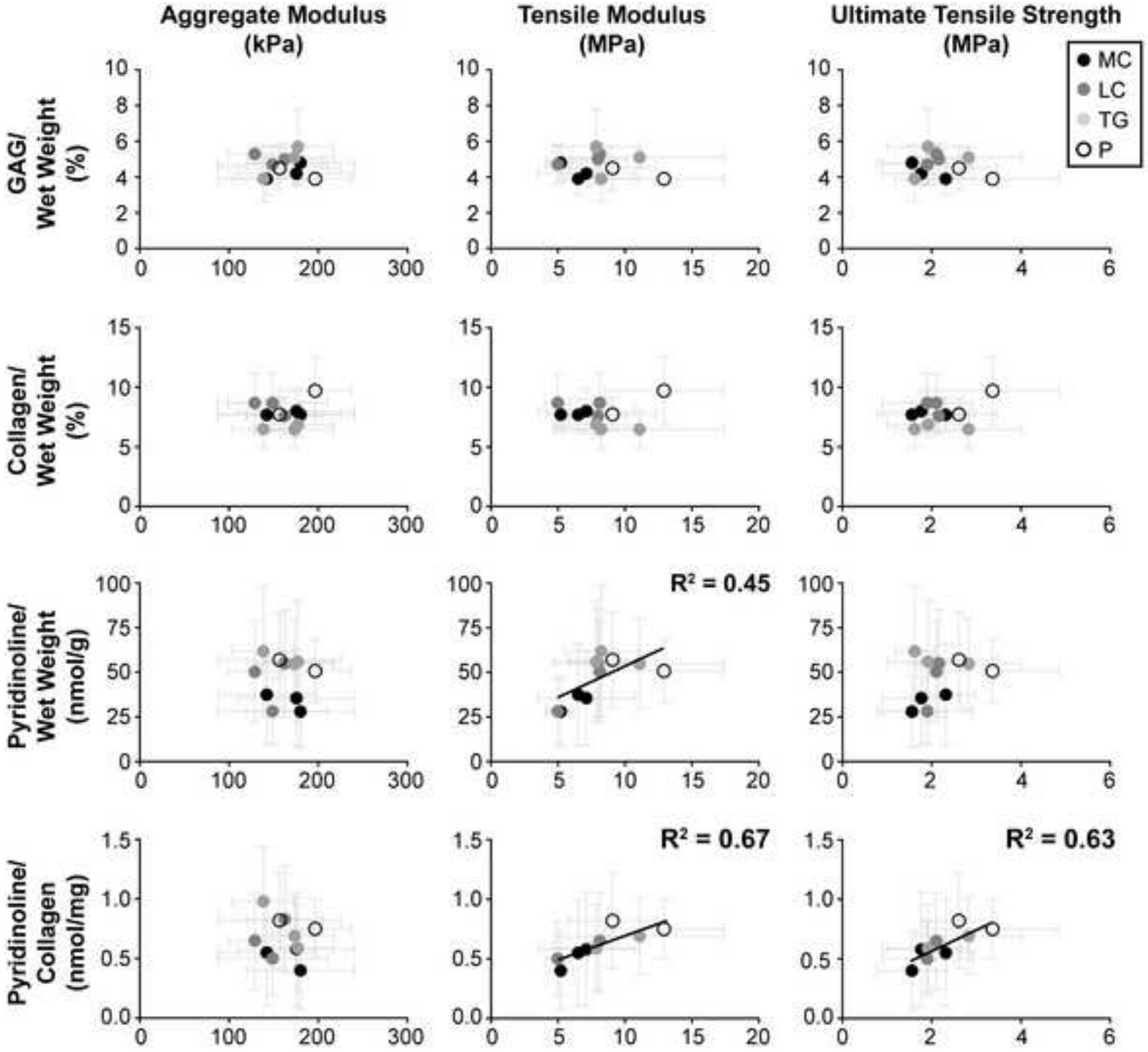

Figure Captions

Figure 1 - Topographical and Regional Overview: Articular cartilage from 11 topographical locations across four regions of the fetal ovine stifle joint was characterized histologically, biochemically, and mechanically.

Figure 2 - Histological and Immunohistochemical Evaluation: Articular cartilage from three locations on the medial condyle (MC), three locations on the lateral condyle (LC), three locations on the trochlear groove (TG), and two locations on the patella (P) of the fetal ovine stifle were stained for GAG, total collagen, collagen I, and collagen II. Vasculature is present in every location. The LC stained most intensely for GAG, followed by the MC, TG, and P. Within each region, the locations with the most intense GAG staining were MC3, LC2, TG1, and P1, respectively. Collagen staining was similar in the MC and LC, but less intense in the P and TG. Within each region, collagen staining was most intense at the MC2, LC2, TG1, and P2 locations, respectively. Collagen I staining was minimal in all locations. All locations stained for collagen II, but the TG and P stained most intensely. Within each region, collagen II staining was most intense at the MC2, LC3, TG1, and P1 locations, respectively.

Figure 3 – Biochemical Characterization: Biochemical contents of the fetal ovine medial condyle (MC), lateral condyle (LC), trochlear groove (TG), and patella (P) are shown in gray. Historical values of biochemical content of juvenile ovine cartilage from the same regions, except for pyridinoline content, are shown in translucent blue (A-D,G,H).[16] Juvenile ovine pyridinoline/WW (E) and pyridinoline/collagen (F) contents, shown in blue, were calculated in this study. The LC contained the greatest GAG/ wet weight (A). The TG contained the greatest

GAG/DNA (B). The P contained the greatest collagen/wet weight (C). There were no regional differences in collagen/DNA (D), pyridinoline/wet weight (E), pyridinoline/collagen (F), or water content (G). The MC contained the greatest DNA/wet weight (H). Topographical biochemical data are available in Table 1.

Figure 4 – Mechanical Characterization: Mechanical properties of the fetal ovine medial condyle (MC), lateral condyle (LC), trochlear groove (TG), and patella (P) are shown in gray. Historical values of biochemical content of juvenile ovine cartilage from the same regions are shown in translucent blue.[16] No regional differences in aggregate modulus (A) or shear modulus (B) were observed. The P was stiffest (C) and strongest (D) in tension. Topographical mechanical data are available in Table 2.

Figure 5 – Structure-Function Correlations: Correlations were tested among mechanical properties and biochemical contents. The aggregate modulus, tensile modulus, and ultimate tensile strength were individually compared to the GAG/wet weight, collagen/wet weight, pyridinoline/wet weight, and pyridinoline/collagen, matched by location. Significant, positive correlations were observed between tensile modulus and both pyridinoline/wet weight and pyridinoline/collagen, as well as between ultimate tensile strength and pyridinoline/collagen.